

## Chapter 3

### High Harmonic Generation from Ions

The highest photon energies obtained from high harmonic generation (HHG) have generally been limited not by the cutoff rule, but by the detrimental effects of ionization when using high laser intensities. The resulting plasma can defocus the laser beam,[59] limiting the peak intensity and therefore  $U_p$ . It also causes a significant phase velocity mismatch between the driving laser and the harmonic light, greatly reducing the harmonic signal. Ionization can be kept to a minimum by using shorter-duration laser pulses or atoms with a large ionization potential, thus allowing the atoms survive to high laser intensities before ionizing. The highest harmonics observed to date, at around 950 eV, have been generated using helium,[15, 70, 67] which has the largest ionization potential of the noble gases. However, helium also has an exceptionally small effective nonlinearity, which limits the harmonic flux. Larger, multi-electron atoms such as argon typically generate greater signals, but the highest observable harmonic orders have been comparatively lower. For example in Ar, photons of greater than 100 eV energy have never been observed using an 800 nm driving laser,[83, 80] even using very short 7 fs duration pulses[65] or large pulse energies. In other work, a longer-wavelength driving laser was used to increase the harmonic emission in Ar to  $\sim 150$  eV.[68] Using longer wavelengths increases the value of  $U_p$  for the same laser intensity, however, this approach also reduces the efficiency of the process since the electron wavefunction is more delocalized, lowering the probability of recombination.

### 3.1 Previous Experiments on HHG from Ions

Harmonic emission from neutral atoms is limited by the saturation intensity, or the intensity at which  $\sim 98\%$  of the atoms are ionized. However, emission from ions can in theory extend to very high energies, since the saturation intensity for each successive stage of ionization is progressively higher. Krause, Kulander, and Schaffer calculated that emission from neutrals and ions is of comparable strength with emission from ions extending to higher energies.[42] In previous experiments, Wahlstrom et al. observed harmonic emission from Ar ions up to  $\sim 100$  eV using an 800 nm driving laser with 250 fs pulse width and 250 mJ of pulse energy focused to an intensity of  $\sim 10^{15}$  W/cm<sup>2</sup>. Their results are shown in figure 3.1. The emission attributed to ions is several orders of magnitude weaker in intensity than the emission from neutral atoms and is still short of the predicted  $I_p + 3.2U_p$  rule.[79, 80]

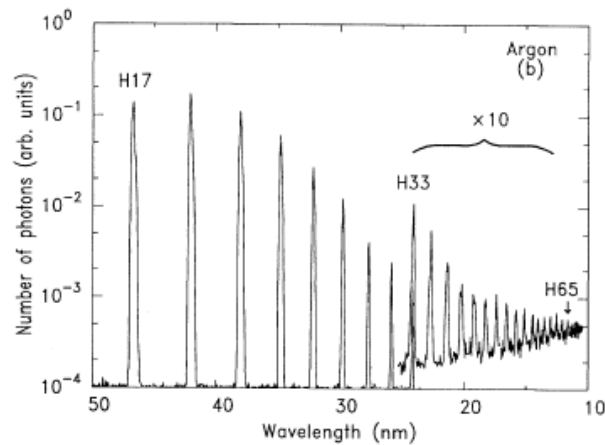


Figure 3.1: Harmonic emission from argon using a gas jet with 250 mJ pulse energy and a 250 fs pulse. From [80]

### 3.2 Experimental Results using Hollow-core Waveguides

In our experiment, high harmonics are generated by focusing intense laser light into a hollow-core waveguide filled with low pressure gas. The waveguide has several advantages over a gas jet. It counteracts the effect of plasma-induced defocusing, allowing high laser intensities to be achieved in a fully ionized gas medium. Also, using a modulated-diameter waveguide, the large phase mismatch associated with ionization can be partially compensated by quasi-phase matching. As a result, we observed harmonic generation from argon up to 250 eV, an extension of 100 eV over previous results using a gas jet setup for HHG. These results demonstrate that emission from ions can greatly increase the photon energies obtainable from HHG and that large ions such as Ar, with high nonlinear susceptibilities compared to He, can be used to generate harmonic emission at energies above 200 eV, in the soft x-ray region of the spectrum.

In our experiment, we use a 1 kHz Ti:sapphire laser system[8] producing 22 fs-duration pulses, with pulse energies of 3 mJ. The laser light is focused into 150  $\mu\text{m}$  inner-diameter, 2.5 cm long, hollow-core waveguides filled with argon. The harmonic emission emerging from the waveguide passes through a zirconium or silver filter to block the fundamental light. Frequency-resolved-optical-gating (FROG) measurements of the laser pulse before and after the fiber filled with low-pressure Ar show some shortening of the pulse from the 22 fs input to 18 fs at the exit due to ionization effects to be discussed in Chapter 5. Care was taken to prevent contamination of the gas by evacuating the waveguide first to  $\sim 10^{-2}$  Torr, and then flowing Ar continuously through it. Figure 3.2 shows the harmonic emission from a straight waveguide filled with 7 Torr of Ar at a peak laser intensity of  $\sim 9 \times 10^{14} \text{ Wcm}^{-2}$ . Under these conditions, the harmonic emission extends up to 180 eV. The falloff in the spectrum toward low energies is a result of the transmission characteristics of the Zr filter used to reject the laser light. Here, we use a 0.4  $\mu\text{m}$  thick Zr filter with 25 nm of Ag coated on one side. When a 0.25 mm-modulated waveguide was used under the same conditions, the highest photon energy observed was the same; however, the signal was 2-3 times stronger.

The laser intensity was determined from the experimentally measured pulse energy and pulsewidth, and is accurate to within 10%. This intensity was also compared with that required to generate the experimentally observed harmonic cutoff, which gives a lower limit for the intensity. Figure 3.3 shows the harmonic emission from Ar at a slightly higher laser intensity of  $1.3 \times 10^{15} \text{ Wcm}^{-2}$  using a waveguide with a periodically modulated diameter.[56] We use a  $0.45 \mu\text{m}$  thick Ag filter that is 5-15% transmissive from around 120 to 385 eV to reject the laser light. In Fig. 3.3, the emission from Ar at this higher intensity now extends up to 250 eV. Note that the increase in observable harmonic order scales linearly with intensity, as expected from the cutoff rule provided that saturation effects do not limit the emission. The signal is clearly emission from HHG since the signal disappears if circularly polarized driving pulses are used.

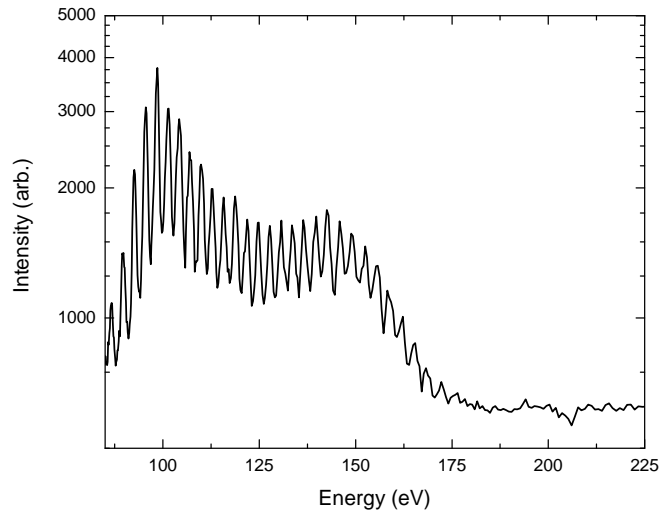


Figure 3.2: Harmonic emission from a straight  $150 \mu\text{m}$  inner diameter, 2.5 cm long fiber filled with low-pressure Ar (7 Torr), driven by an 800 nm laser with an 18 fs pulse duration and a peak intensity of  $9 \times 10^{14} \text{ Wcm}^{-2}$ . The spectrum was taken using the SC grating and an exposure time of 300 s.

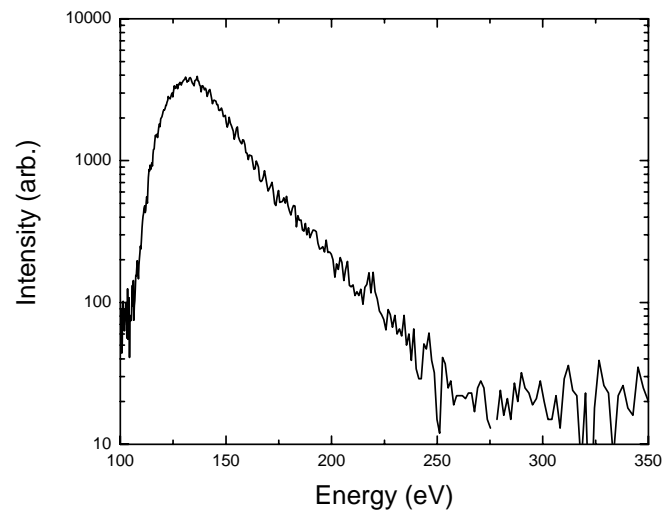


Figure 3.3: Harmonic emission at a higher peak laser intensity of  $1.3 \times 10^{15} \text{ Wcm}^{-2}$ , using a 0.25 mm period modulated waveguide. The spectrum was taken using the SC grating with a 600 s exposure time.

### 3.3 Evidence for Harmonic Emission from Ions

The laser intensities required to generate the highest harmonics shown in Figs. 3.2 and 3.3 are above the saturation intensity for neutral Ar atoms of  $7.5 \times 10^{14} \text{ Wcm}^{-2}$ , for an 18 fs laser pulse duration. Thus, we attribute the highest observed harmonics, in the energy range from  $\sim 160 \text{ eV}$  to  $250 \text{ eV}$ , to emission from Ar ions. To illustrate this, Fig. 3.4 shows the calculated population fractions of Ar, Ar+, and Ar++ as a function of time during the laser pulse at a peak laser intensity of  $1.3 \times 10^{15} \text{ Wcm}^{-2}$ , and for a laser pulsewidth of 18 fs. These parameters correspond to the experimental conditions of Fig. 3.3. This calculation was done using the well-established Ammosov-Delone-Krainov (ADK) ionization rates, given in more detail in appendix A.[3] The left axis gives the population fractions for the various species. The right axis plots the HHG cutoff calculated from the cutoff rule for the laser intensity profile. In this calculation,  $h\nu_{max} = I_p + 3.17U_p$ , where  $I_p$  is the ionization potential Ar of 15.8 eV, and where the instantaneous laser intensity is used to calculate  $U_p$ . (Note that  $I_p$  for Ar+ is 27.6 eV, which would shift the harmonic energies slightly higher for the emission from ions). At a laser intensity of  $\sim 7.7 \times 10^{14} \text{ Wcm}^{-2}$ , Ar is fully ionized, and the highest observable harmonics from the neutral atoms should therefore be approximately 160 eV. At the same laser intensities where the population of Ar neutrals is zero, the population of singly ionized Ar+ ions is significant. Figure 3.5 shows the ionization rates multiplied by population at a given time during the driving pulse for Ar and Ar+. Near the peak of the pulse, the rate for Ar+ dominates and therefore is the source of the HHG emission. Note that in this analysis, the assumed 18 fs pulse width is conservative; if the laser pulse is longer, full ionization of neutrals occurs at even lower laser intensities in the pulse and therefore strengthens the argument for emission from ions. The laser pulse cannot be shorter than 18 fs because of spectral bandwidth limits. Finally, the same arguments can be used for the lower intensity data corresponding to Fig. 3.2 - the higher harmonics must be emitted from ions, because Ar is fully ionized well before the peak of the pulse.

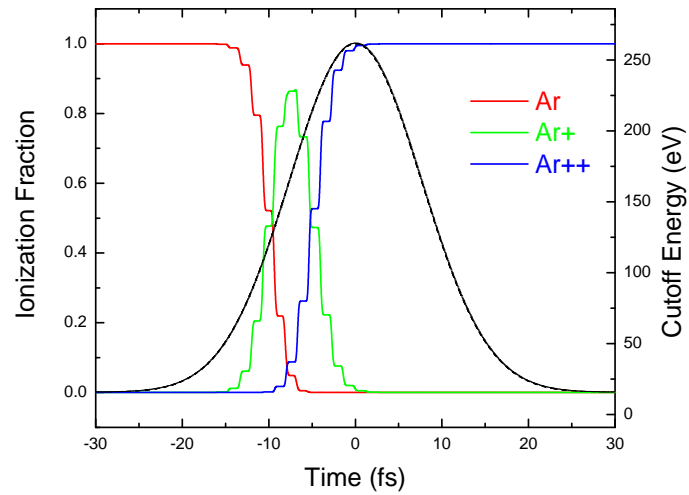


Figure 3.4: Calculated ionization levels in argon for an 18 fs laser pulse at a peak laser intensity of  $1.3 \times 10^{15} \text{ Wcm}^{-2}$ , using ADK rates. Laser pulse (black dashed); Ar (red); Ar+ (green); Ar++ (blue). The right axis shows the predicted HHG cutoff energy for the laser intensity profile, calculated from the cutoff rule.

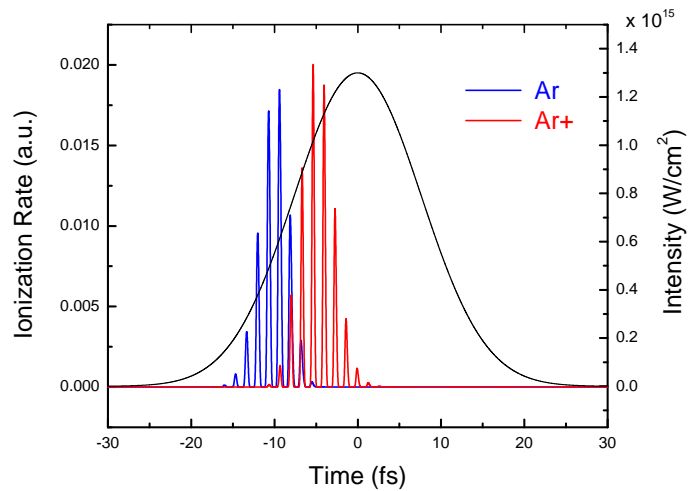


Figure 3.5: Calculated ionization rates of argon species for the same conditions as in Fig. 3.4.

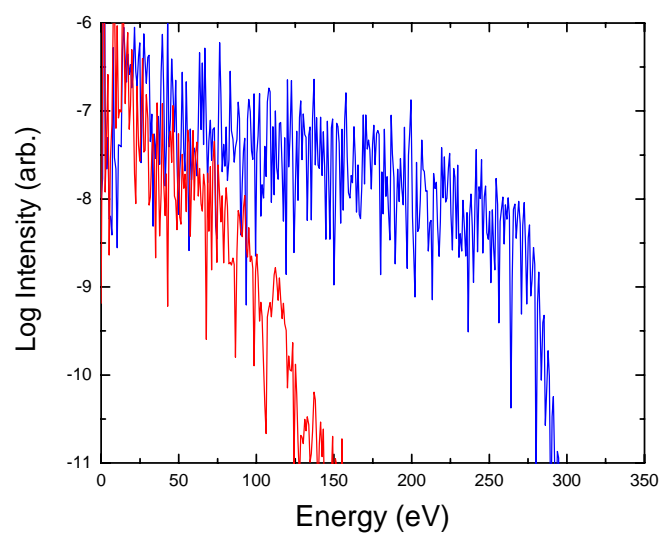


Figure 3.6: Calculated harmonic emission from neutral (red) and singly ionized Ar (blue) for an 18 fs laser pulse centered at 800 nm, at a laser intensity of  $1.3 \times 10^{15} \text{ Wcm}^{-2}$ . The ion spectrum has not been corrected for the dynamically varying populations.

As further evidence for HHG from ions, we can compare the observed spectra with the predictions of a fully quantum single-active electron approximation model that uses a soft core potential to fit the ionization potential of the atom or ion under consideration.[37, 20] Only qualitative comparisons are possible since the theory does not account for propagation effects or the changing fraction of ionized species. Figure 3.6 shows predictions of the quantum model for the harmonic spectrum emitted by Ar and Ar+ for an 18 fs driving-laser pulse at a peak intensity of  $1.3 \times 10^{15} \text{ Wcm}^{-2}$ . The model predicts strong emission from neutrals up to photon energies of 125 eV. For higher harmonics, the intensity drops rapidly by many orders of magnitude with increasing harmonic order due to the complete ionization of Ar neutrals. In contrast, emission from Ar+ is much stronger up to 260 eV. These theoretical predictions are in very good qualitative agreement with our experimental observations. We also note that the quantum calculations predict comparable emission intensities (i.e. effective nonlinear susceptibilities) for neutrals and ions. This is consistent with our observations, which do not show a large discontinuity in emission intensity with higher harmonic orders.

### 3.4 Validity of the ADK Model in the BSI Regime

One important question to address is whether the ADK model, which is valid in the tunnelling ionization regime, is applicable in the barrier suppression ionization (BSI) regime. Barrier suppression occurs when the electric field strength is comparable or greater than the strength of the binding potential of the atom, allowing the electron to escape directly from the potential well without tunnelling. This would lead to inaccuracies in the predictions of Figs. 3.4 and 3.5, although the quantum rate calculations and their predictions shown in Fig. 3.6 are valid in this regime. Barrier suppression of an atom occurs for a field strength of  $E_{bs} = I_p^2/4$ , or, in the case of Ar, an intensity of  $2.5 \times 10^{14} \text{ Wcm}^{-2}$ . [41, 5] Previous theoretical work has shown that in this regime, ADK theory may overestimate the ionization rate and thus underestimate the cutoff harmonic order from neutrals.[66, 71] Figure 3.7 shows the static field ionization rates for H and He from a numerical solution of the time-dependent Schroedinger equation and from

ADK theory. Above the barrier suppression field strength, ADK begins to overestimate the rate. However, when calculating the total ionization over the pulse, the error is less because only the peak of the pulse has an intensity in the BSI regime. In Figure 3.8, the total amount of ionization of H is calculated as a function of peak electric field amplitude and pulse duration. As expected, for a shorter duration pulse, the error in the total amount of ionization is greater since a higher proportion of the pulse is at the BSI intensity.

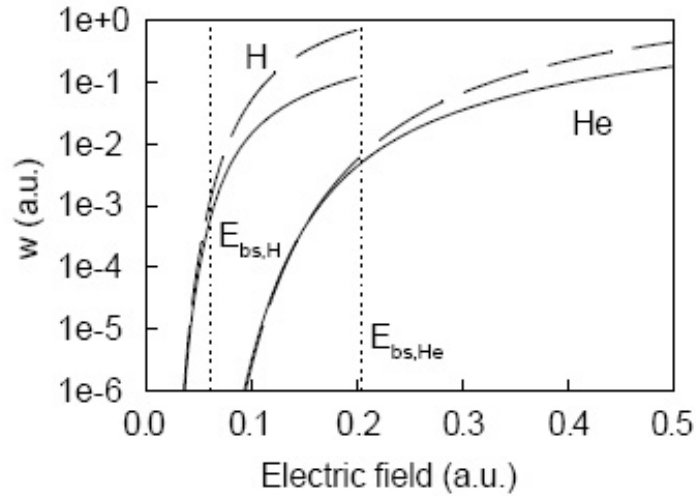


Figure 3.7: Static ionization rates of H and He versus electric field strength. Solid line: numerical calculations of TDSE. Dashed line: ADK theory. From [66].

Another source of error can result from the fact that the ADK theory describes a DC tunnelling rate. In the quasi-static approximation (QSA), these rates can be applied to oscillating electric fields if the tunnelling time is less than the oscillation period, or when the Keldysh parameter,  $\gamma \leq 1/2$ , where

$$\gamma = \left(\frac{I_p}{2U_p}\right)^{1/2} = \sqrt{2mI_p\omega_0}/E. \quad (3.1)$$

However, A. Scrinzi et al. [66] point out that in the BSI regime,  $\gamma_{bs} = 16\omega_0/(2I_p)^{3/2}$ , which for 800 nm light and noble gas atoms (Kr, Ar, Ne, He) ranges between  $\gamma \approx 0.5 - 2$ , so that the quasi-static approximation may not be valid. By comparing numerical calculations with calculations using the QSA of the total amount of ionization produced from a pulse, they find

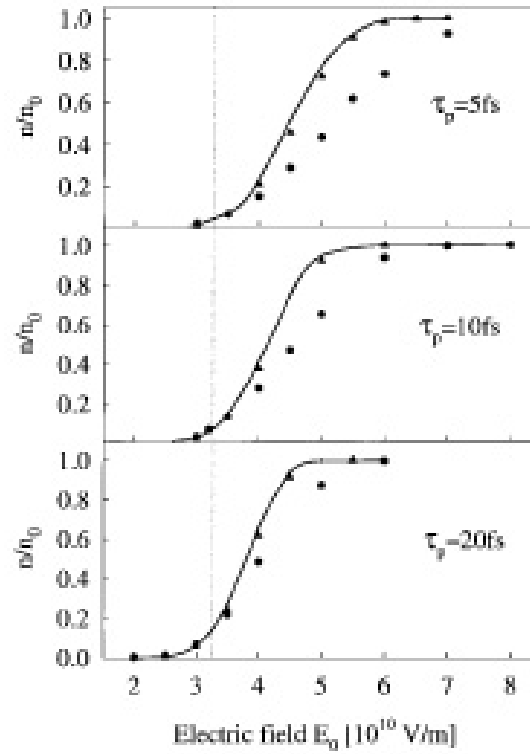


Figure 3.8: Fraction of ionized H in the BSI regime as a function of the peak electric field amplitude for pulses of 5, 10, and 20 fs in duration. Full line is ADK model, triangles show Krainov model, and circles show time-dependent Schrodinger equation. The dotted line is  $E_{bs}$  for H. From [71].

that the deviation is less than 5% when the Keldysh parameter is between  $0.5 < \gamma < 2$  for 800 nm light. They conclude that the Keldysh condition which is calculated assuming tunnelling ionization is not the same as for the BSI regime.

In our experiments, we use an 18 fs duration pulse with a peak intensity of  $1.3 \times 10^{15}$  Wcm<sup>-2</sup>. The peak electric field amplitude is  $E_p = 2.3E_{bs}$  for argon; however, the peak field that the neutral argon atoms survive to will be somewhat less. From the calculations for He, the actual rate is about 80% what ADK theory predicts when the field is twice the barrier suppression field. Therefore the error in the ADK calculation of the total ionization fraction during the pulse should not be significant. For Ar+, the calculated ionization rate using the ADK model should be accurate, since we are below the barrier suppression intensity of the ion ( $2.4 \times 10^{15}$  Wcm<sup>-2</sup>) for our peak intensities. Previous work has shown very good agreement between experiment and theory using ADK ionization rates for ions.[81, 17] Therefore, it is valid to conclude that the significant extension of HHG we observe in Ar is due to emission from ions.

### 3.5 Plasma-induced Defocusing

We attribute our ability to observe these very high harmonic orders in argon primarily to the use of a waveguide for high harmonic generation.[50] The waveguide minimizes the effect of laser beam defocusing, resulting in high driving laser intensities even in the presence of a substantial plasma. Theoretical calculations[59] and experimental observation[2] show that plasma-induced defocusing effects limit the maximum intensity that can be achieved when a laser is focused into an ionizing gas. These effects become significant when the defocusing length, defined in Ref.[59] as  $l_D = \lambda n_c / 2n_e$ , where  $n_e$  is the electron density and  $n_c$  is the critical density, is smaller than the confocal parameter. In effect, the spatially varying plasma creates a negative lens and the defocusing length is the length at which the phase advance at the center of the beam is  $\pi/2$ . Under the conditions in our experiment, 100% ionized gas at 7 Torr, the defocusing length is around 1 mm. This is an order of magnitude shorter than the laser beam confocal parameter of  $\sim 1$  cm, and indicates that without the waveguide, the ionizing

gas would defocus the pulse before reaching its peak intensity. Experimentally, we observe that the transverse profile of the beam emerging from a 2.5 cm long waveguide is unaffected by the presence of the ionized gas for argon pressures up to 7 Torr, and that the energy decreases by 10-15%. This energy loss corresponds to a deposited energy of  $\sim 30$  eV for each atom in the waveguide, and will lead to double-ionization of atoms in the center of the waveguide. We also observe a significant spectral broadening, blueshifting of around 20-50 nm, and a shorter pulse duration (from 22 fs to 18 fs) of the driving laser pulse when the gas is present, all of which are indicative of a strong laser-plasma interaction that would be enhanced with guiding. At the high laser intensities and ionization levels present in the waveguide, spectral broadening of the harmonic peaks can also occur, as seen in Fig. 3.3.

When the argon pressure is increased above 9 Torr, the output mode breaks up and harmonics are no longer observed. Therefore, there exists a limit to the amount of ionization-induced defocusing for which the waveguide can compensate. Experimentally, we observe that reducing the gas pressure in the waveguide will lead to an increase in the highest observed photon energy. Figure 3.9 shows HHG spectra for argon at 5 and 7 Torr in a straight waveguide. At the lower pressure, the flux at lower photon energies is reduced, but the higher photon energies are enhanced. Figure 3.10 shows a more dramatic result for harmonics from neon at the same intensity. There are several possible explanations for these results. It is possible that there is still some defocusing effect which increases with higher pressures, reducing the intensity. Also, at higher gas pressures, the laser energy at the output of the fiber is reduced, either from ionization or from other loss mechanisms in the waveguide. The reduction in laser energy and therefore intensity could also explain the decrease in harmonic energy.

The ability to generate harmonics in highly ionized media and from atomic ions holds great promise to advance the energy range and flux of soft x-ray sources from HHG. Previously, it was believed by many in the field that the limit to HHG energy was the saturation intensity. In this work, we demonstrate that the true limit is given by the cutoff rule. In Chapter 2, it was shown that the flux can be enhanced by using modulated waveguides even in 100 % ionization.

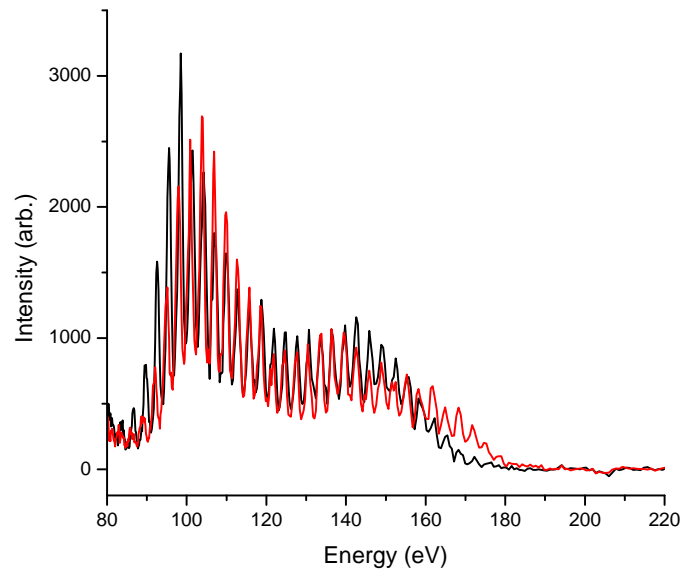


Figure 3.9: Measured harmonic spectra from a straight waveguide filled with argon at 5 Torr (red) and 7 Torr (black) for a pulse peak intensity of  $\sim 9 \times 10^{14} \text{ Wcm}^{-2}$ . Both spectra taken with the SC grating and an exposure time of 300 s (using  $0.4 \mu\text{m}$  thick Zr filters).

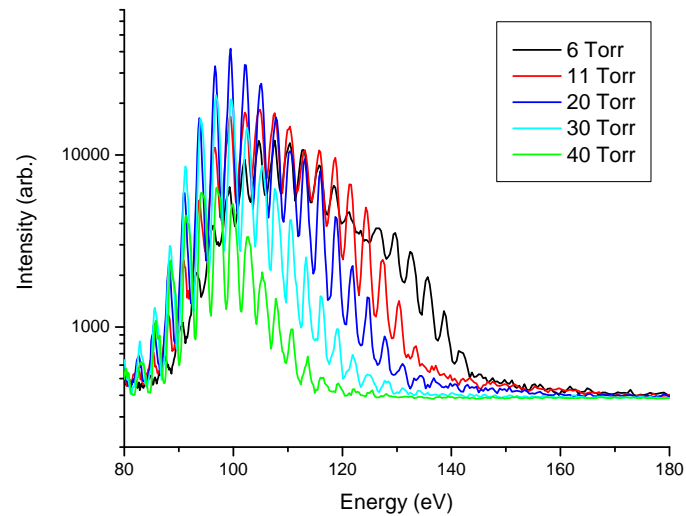


Figure 3.10: Harmonic spectra from a straight waveguide filled with Ne at different pressures for a peak laser intensity of  $\sim 9 \times 10^{14} \text{ Wcm}^{-2}$ . All spectra taken with the SC grating and a 10 s exposure (using  $0.4 \mu\text{m}$  thick Zr filters).

For the results shown in Fig. 3.3, the falloff in the emission at higher energies is likely due to the rapidly decreasing coherence length at higher levels of ionization, from  $\sim 0.5$  mm at 100 eV to  $\sim 50$   $\mu\text{m}$  at 250 eV. Although a 0.25 mm modulated waveguide was used, the process was not optimally phase matched and further enhancement of the flux is expected by using shorter modulation periods and longer waveguide lengths.